A Rotamer Library to Enable Modeling and Design of Peptoid Foldamers

P. Douglas Renfrew,[†,⊥] Timothy W. Craven,[†,⊥] Glenn L. Butterfoss,[∥] Kent Kirshenbaum,[‡] and Richard Bonneau*[,†,§]

[†]Center for Genomics and Systems Biology, Department of Biology, [‡]Department of Chemistry, and [§]Courant Institute of Mathematical Sciences, Computer Science Department, New York University, New York, New York 10003, United States

[∥]Center for Genomics and Systems Biology, New York University Abu Dhabi, Abu Dhabi, United Arab Emirates

Ⓢ *Supporting Information*

ABSTRACT: Peptoids are a family of synthetic oligomers composed of N-substituted glycine units. Along with other "foldamer" systems, peptoid oligomer sequences can be predictably designed to form a variety of stable secondary structures. It is not yet evident if foldamer design can be extended to reliably create tertiary structure features that mimic more complex biomolecular folds and functions. Computational modeling and prediction of peptoid conformations will likely play a critical role in enabling complex biomimetic designs. We introduce a computational approach to provide accurate conformational and energetic parameters for peptoid side chains needed for successful modeling and design. We find that peptoids can be described by a "rotamer" treatment, similar to that established for proteins, in which the peptoid side chains display rotational isomerism to populate discrete regions of the conformational landscape. Because of the insufficient number of solved peptoid structures, we have calculated the relative energies of side-chain conformational states to provide a backbone-dependent (BBD) rotamer library for a set of 54 different peptoid side chains. We evaluated two rotamer library development methods that employ quantum mechanics (QM) and/or molecular mechanics (MM) energy calculations to identify side-chain rotamers. We show by comparison to experimental peptoid structures that both methods provide an accurate prediction of peptoid side chain placements in folded peptoid oligomers and at protein interfaces. We have incorporated our peptoid rotamer libraries into ROSETTA, a molecular design package previously validated in the context of protein design and structure prediction.
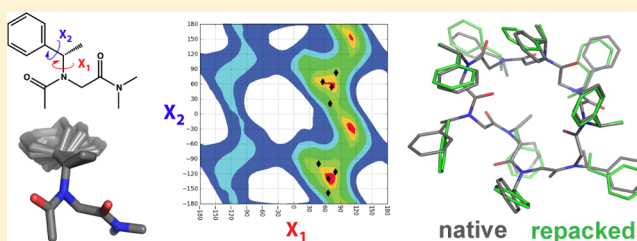
■ INTRODUCTION

Sequence-defined biopolymers, such as proteins and nucleic acids, incorporate backbone and side-chain constituents that endow these macromolecules with the ability to fold into well-defined secondary and tertiary structures. The complexity and functionality of these folded biopolymers has spurred intensive research toward a predictive understanding of the relationships between their sequences, structures, and functions. Computational strategies to engineer proteins and nucleic acids have matured to the point where de novo design of elaborate new protein and nucleic acid structures can be conducted with some reliability.[1−3] The development of computational tools for the design of proteins also provides a valuable blueprint for building analogous tools to enable design of other abiotic folded oligomeric systems, termed foldamers.[4] A key component of many protein design programs is the discretization of side-chain degrees of freedom by representing side chains as conformational isomers, termed "rotamers".[5] Here we describe general methods to build rotamer libraries for peptidomimetic foldamers, and apply these methods specifically to a family of peptoid foldamers composed of N-substituted glycine monomers. In this way, we aim to remove a fundamental roadblock and enable design methods for diverse foldamers incorporating abiotic monomer types.

Foldamers are a class of oligomeric molecules for which noncovalent interactions dictate the self-organization of stable secondary and tertiary structures.[4] There is now a veritable bestiary of foldamer species and hybrids.[6−11] A large community of researchers are actively developing functional peptoids to address a diverse set of goals.[12−15] The intensity and diversity of these efforts punctuates the need for general computational tools to aid in the pursuit of many complex design tasks. In this study, we provide the computational tools and develop the theoretical background necessary to design the next generation of folded and functional peptoid oligomers.

The solid phase submonomer peptoid synthesis protocol introduced by Zuckermann et al.[16] facilitates the introduction of a myriad of side-chain types by utilization of readily available primary amines as synthons. Over 230 different peptoid side chains have now been described in the literature.[17] Peptoids have been the subject of considerable research aimed at developing sequence−structure[18−20] as well as structure−

function[9,21−24] relationships. These efforts have established that peptoids can populate a range of secondary structure types and that peptoids exhibit strong interactions between side chain and backbone degrees of freedom. Despite the absence of stabilizing backbone hydrogen-bonds, peptoids have been shown to fold, and their folds can be predictably controlled by variation of the monomer sequence to achive a desired functionality.[25−30] Additionally, new native chemical ligation strategies have been developed to ligate peptoids to peptides.[31] This ligation protocol will enable the synthesis of hybrid biomacromolecules aimed at achieving advanced functions.

Rotamer libraries are an essential part of the protein design toolbox.[5] Based upon the observation that protein side chains populate distinct areas of side-chain dihedral angle conformation space and that dihedral angle conformations are in some cases strongly dependent on the adjacent ϕ and ψ backbone dihedral angles,[32,33] side-chain conformations have been grouped together into bins that represent frequent rotational-isomers and given the moniker "rotamer". For canonical amino acids (CAAs), methods to find these regular clusters of conformations rely on statistical analysis of the Protein Data Bank (PDB). The large number of structures for each side chain across the spectrum of allowed backbone dihedral angles allows for the determination of relative rotamer energies by fitting a Boltzmann distribution to the population of side-chain conformations. Current rotamer libraries are backbone dependent: given ϕ and ψ backbone torsion angles, the rotamer library specifies a set of allowable rotamers, the estimated probability of each rotamer, and some measure of the deviation within the cluster of similar conformations represented by that rotamer. Enumerating the set of side-chain conformations and their likelihoods allows for rapid searching of low energy side-chain conformation in discrete steps. These libraries are key constituents in several structural bioinformatics approaches including methods for placing side chains on homology models, protein structure prediction, and protein design.

Statistically derived rotamer libraries are not feasible for systems with few experimental structures. In the case of peptoids, there are fewer than 20 experimentally determined high-resolution peptoid structures, the largest of which includes only 16 residues. This limitation necessitates the use of MM based force-field energy calculations and QM calculations to derive estimates for the relative conformer energies of peptoid foldamers. From these computed estimates, we can then establish a rotamer-like treatment of side-chain probabilities. Previous attempts at developing rotamer libraries for non-canonical α-amino acid[34,35] and β-amino acid side chains[36] have also used MM-based force-fields.

There are many conceivable algorithmic options to determine rotamer minima placement. In this study, we devised two distinct rotamer library development methods and find they achieve similar levels of quality in structure prediction and design task performance. We evaluated the quality of these rotamer libraries within the context of the molecular modeling suite ROSETTA.[37] In addition to creating rotamer libraries for peptoids, we introduce several substantial modifications to the ROSETTA code to enable design with noncanonical backbone chemistry. ROSETTA was initially built to predict protein function, but has been expanded to include protocols for docking, protein design, RNA structure prediction, and other macromolecular structure and design tasks. The code is widely distributed and used by more than 1500 research groups worldwide. By incorporating our work on peptidomimetic

design into ROSETTA, we make available a large number of computational protocols for scoring, kinematics (moving the backbone), docking, and optimization. This enables utilization of peptoids in existing ROSETTA design protocols, such as designing peptoid sequences to interact with proteins.
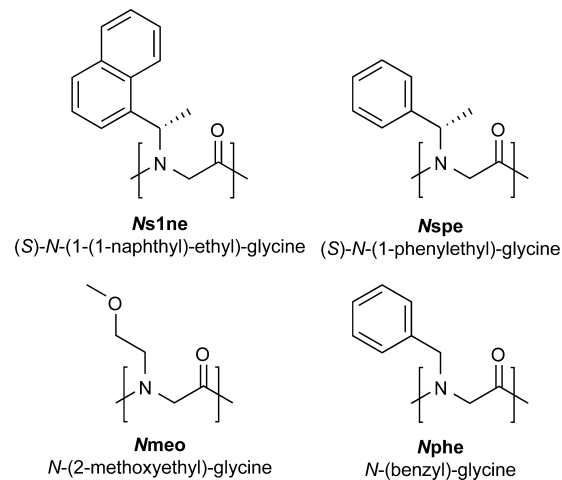
■ METHODS

Below we describe the methods used for the creation of rotamer libraries, methods used to evaluate the assumptions made in utilizing rotamers, as well as methods used to characterize the performance of the resultant rotamer libraries. Additional methods are detailed in the Supporting Information.

Selection of Structures and Side Chains. We have recently compiled a database of all high-resolution peptoid structures (the Peptoid Data Bank[38]). A subset of these structures was chosen for characterizing our rotamer libraries. We additionally included structures of peptoid/peptide hybrids bound to SH3 and WW domains.[23,24] Selection criteria and modifications to structures are detailed in the Supporting Information.

In the set of oligo-peptoid structures, there are 9 different peptoid side chains, at 87 positions and with 93 unique conformations. Four of the most commonly observed peptoid side chains (Nspe, 21; Nmeo, 17; Nphe, 15; Ns1ne, 11), making up 69% of unique conformations in the Peptoid Data Bank, are described in the main body of the text and are shown in Scheme 1. Side chains for which fewer experimental examples exist (Nary, 16; Nrch, 5; Npe, 4; N1nap, 3; Nrpe, 1) are detailed in the Supporting Information.

Scheme 1. Four of the Most Common Side Chains in Peptoid Structures

Ns1ne
(S)-N-(1-(1-naphthyl)-ethyl)-glycine

Nspe
(S)-N-(1-phenylethyl)-glycine

Nmeo
N-(2-methoxyethyl)-glycine
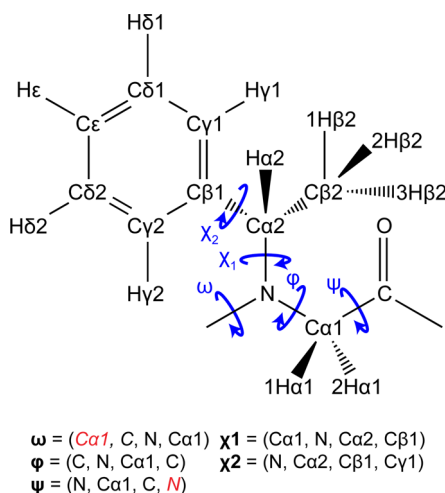
Nphe
N-(benzyl)-glycine

In addition to the 9 side chains mentioned above, we chose 45 side chains to include within the ROSETTA framework, based on their prevalence in the literature and the ease with which they could be incorporated into oligomers via standard synthetic routes.[16] A full list of the 54 peptoid side chains that were incorporated into ROSETTA and for which we created rotamer libraries are shown in Figures S1−S7.

Atom, Torsion Angle, and Rotamer Nomenclature. Previous studies of oligo-peptoid structures have defined both atom names and dihedral angles in different ways. Our choice of atom names was strongly influenced by peptide atom naming for compatibility with protein modeling programs and is similar to that used by Huang and co-workers.[39] The most notable difference is the definition of the χ_1 torsion angle. Whereas previous studies have defined the χ_1 dihedral angle relative to the preceding carbonyl carbon, ROSETTA requires that the atoms that define a χ dihedral angle be contained within the residue unit.[40] We therefore deviated from past work[41] by defining χ_1 with respect to the Cα1 atom (Cα in peptides). Our atom name and

torsion angle naming conventions[42] are shown for an *N*spe residue in Scheme 2.

Scheme 2. Side Chain and Backbone Atom and Torsion Naming for (*S*)-*N*-(1-Phenethyl)-glycine (*N*spe)[a]
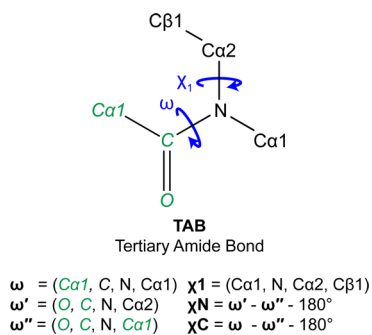

ω = (*Cα1*, C, N, Cα1) $\chi1$ = (Cα1, N, Cα2, Cβ1)
φ = (C, N, Cα1, C) $\chi2$ = (N, Cα2, Cβ1, Cγ1)
ψ = (N, Cα1, C, *N*)

[a]Atom names shown as red italics in torsion angle definitions are atoms in the preceding (ω) or following (ψ) residues in a oligo-peptoid chain and not shown in scheme.

In our analysis of peptoid side chain conformations below, we use the rotamer notation originally set forth by Lovell et al. for its clarity and brevity, where **p** is used to represent "plus" (*gauche+*, 60°), **m** for "minus" (*gauche−*, −60°), and **t** for "trans" (*trans*, 180°).[43] For side chains with dihedral angles that are commonly found at angles other than −60°, 60°, or 180°, the angle is shown in the notation. When referring to the χ_1 rotamer wells, unless otherwise noted, we use **m** and **p** to refer to −90° and 90°, respectively (e.g., a side chain listed with a rotamer of **mm** would have a χ_1 dihedral angle near −90° and a χ_2 dihedral angle near −60°, while an **m90°** rotamer would have a χ_1 dihedral near −90° and a χ_2 dihedral near 90°).[44]

Evaluation of Peptoid Side Chain Conformation Dependence on the Preceding-ω Dihedral Angle. QM energy landscapes of χ_1, χ_N, and χ_C as a function of the preceding-ω dihedral in the context of a tertiary amide bond (TAB) model (Scheme 3) were computed. The TAB model contains the minimum set of atoms needed to simultaneously describe the preceding-ω and χ_1 dihedral angle of an oligo-peptoid residue. All QM geometry optimizations and single point energy calculations of TAB models were evaluated at the B3LYP/6-311+G(d,p) level of theory using GAUSSIAN09.[45]

Scheme 3. Tertiary Amide Bond (TAB) Model, Torsion Angle, and Dunitz Parameter Definitions[a]

TAB
Tertiary Amide Bond

ω = (*Cα1*, C, N, Cα1) $\chi1$ = (Cα1, N, Cα2, Cβ1)
ω' = (O, C, N, Cα2) χN = ω' - ω'' - 180°
ω'' = (O, C, N, *Cα1*) χC = ω - ω'' - 180°

[a]Atoms are named as in Scheme 2, and names shown as green italics represent atoms from preceding residues in a oligo-peptoid chain.

Two sets of TAB models were constructed that combinatorially sample the ω dihedral angle and the χ_1 dihedral angle when the ω dihedral is in either a *cis* or *trans* conformation. The set of *cis*-ω input TAB models sampled ω from −40° to 40 in 10° intervals. The set of *trans*-ω input TAB models sampled ω from −140° to 140° in 10° intervals. Both sets of TAB model inputs sample the χ_1 dihedral angle through a full rotation in 10° intervals. Each instance was optimized, keeping the ω and χ_1 dihedral fixed.

Two additional sets of TAB model inputs were constructed to quantify the changes in the location of the energy minima. These additional sets sample the same *cis* and *trans* ranges but set χ_1 to 90° or −90°. Both sets of inputs were subjected to QM geometry optimization where only the ω dihedral angle values were fixed followed by a single point energy calculation. The calculations of the ω versus χ_C and ω versus χ_N energy landscapes are detailed in the Supporting Information. The results are shown in Figures 2 and S8.

Side-Chain Energy Landscape Calculations of Fixed-Backbone Models of Four Common Side Chains. To compare the QM based energy landscape to the ROSETTA **mm_std**[34] (a MM-based force-field) based energy landscape, we calculated the energy landscapes for four of the most common side chains in the context of both backbone-independent (BBI) and backbone-dependent (BBD) model compounds (Scheme 4). The BBI model was used to

Scheme 4. Backbone-Independent (BBI) (left) and Backbone-Dependent (BBD) "dipeptoid" (right) Models Used in the Rotamer Library Creation Protocols

BBI
Backbone Independent

BBD
Backbone Dependent "Dipeptoid"
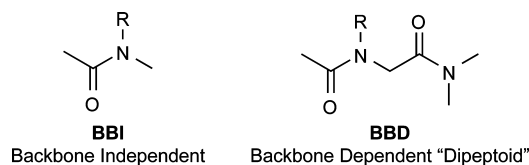
quantify the ω dependence of side-chain energy landscapes. Models were initialized at 10° intervals for each χ angle, keeping ω and the other χ dihedral angles fixed. All other parameters were allowed to optimize. To further quantify the concerted effects that ω, ϕ, and ψ might have on the energetic landscape, we repeated the χ dihedral scan on the BBD model system while keeping the ω, ϕ, and ψ angles fixed at 0°, −90°, and 180°, respectively, as a majority of peptoid structures have these approximate backbone dihedral configurations. All QM geometry optimizations and single point energies were evaluated at the B3LYP/6-311+G(d,p) level of theory using GAUSSIAN09.[45] Similar energy scans were repeated with the same model compounds using the ROSETTA **mm_std** force-field without geometrical optimization. The results are shown in Figure 3.

Rotamer Library Creation. We have previously shown that using the MM-based **mm_std** energy function in ROSETTA, we can produce rotamer libraries for proteins and noncanonical α-amino acids that are comparable to statistically derived rotamer libraries.[34] To explore and compare the relative merits of context and scoring approximations we describe two methods: (1) quantum mechanically seeded (QMS): which uses a highly accurate QM based scoring function, but a minimal model of the peptoid backbone/environment, and (2) k-means clustering (KMC): which uses a more efficient molecular mechanics scoring function, but more extensively explores a model of the peptoid backbone. Neither method utilizes experimentally determined oligo-peptoid structures to determine rotamer positions.

Both protocols require a **ResidueType** parameter file that instructs ROSETTA how the side chain is allowed to move and how the energy of the residue is to be calculated. Drew et al. present a detailed description of **ResidueType** parameter file creation for diverse peptidomimetics.[40] The **ResidueType** parameter file describes the atom names and types, the chemical connectivity of the side chain and an "ideal" internal-coordinate representation used when ROSETTA needs to create new instances of the side chain. A QM geometry optimization of a BBD "dipeptoid", using GAUSSIAN09 at the

B3LYP/6-311+G(d,p) level of theory, is used to generate the idealized internal coordinates that serve as a starting point for the KMC and QMS protocols.

K-Means Clustering Method. Our previously described rotamer library construction protocol[34] was adapted for peptoids as shown in Figure 1. The rotamer calculations were performed on a BBD
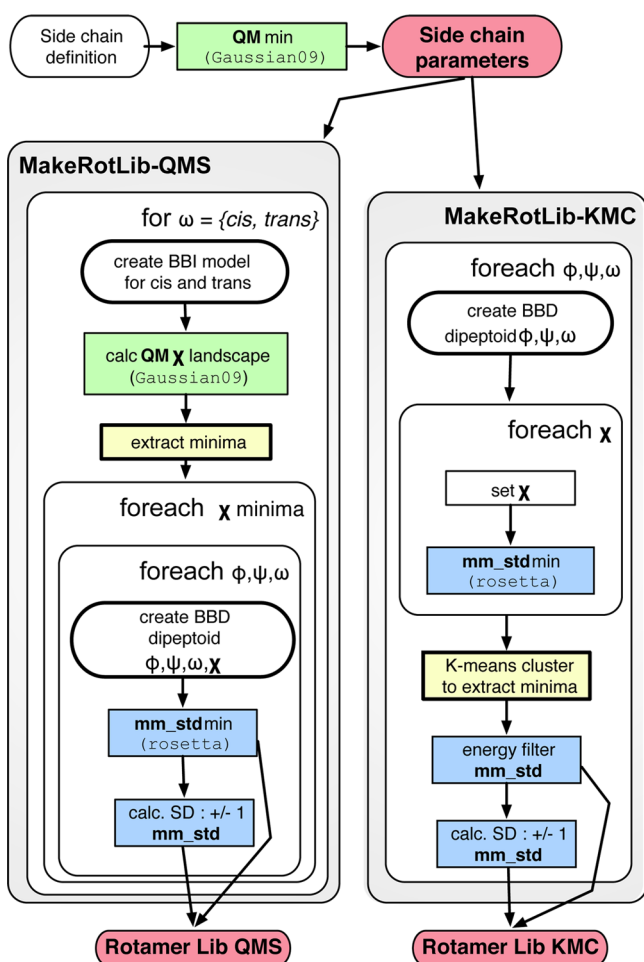

Figure 1. Workflow for the k-means clustering (KMC) and quantum mechanically seeded (QMS) rotamer library construction protocols. Boxes shaded in green are QM geometry optimizations of backbone-dependent (BBD) or backbone-independent (BBI) models; red, inputs to ROSETTA; blue, geometry optimization using the ROSETTA **mm_std** energy function; yellow, identification of local energy minima. A more detailed explanation can be found in the main text.

"dipeptoid" model system (Scheme 4). The "dipeptoid" model system, a peptoid residue with an acetylated N-terminus and a N-dimethylamide C-terminus, has been previously used to examine backbone-side-chain interactions in peptoids[41,44] as it mimics the environment of the side chain with its own backbone and the backbones of the preceding and following residues. The additional dependence of peptoid side chain conformations on the preceding-ω backbone dihedral angle necessitated modification to the protocol to sample and produce rotamer libraries that are dependent on the preceding-ω angle as well as ϕ and ψ dihedrals. The ϕ and ψ backbone dihedrals were sampled through a complete rotation in 10° intervals to produce 36 ϕ and 36 ψ bins. In the set of ROSETTA compatible Peptoid Data Bank structures, *cis* and *trans* ω dihedral angles range from −20.5° to 20.1° and −162.1° to 151.4° respectively. Preceding-ω backbone dihedrals were sampled between −30° to 30° and −150° to

150° in 10° intervals to produce 14 ω bins. A combinatorial sampling of all ω,ϕ,ψ bins yields 18 144 backbone bins.

For each backbone bin, "dipeptoids" were constructed that combinatorially sample the side-chain dihedral angles. Side-chain dihedral angles were sampled at user-defined sets of angles relating to the number of χ angles, the chemical connectivity and the expected number of rotamers; typically 10° intervals (e.g., Nspe has 36 χ_1 and 36 χ_2 samples to produce 1296 "dipeptoids" for each ω,ϕ,ψ bin). The "dipeptoids" were then optimized with a linear-gradient minimization until convergence. The ω, ϕ and ψ dihedrals were fixed during the minimization. The set of minimized "dipeptoids" was then k-means clustered based on the similarity of the minimized side-chain dihedral angles. The final rotamers for a given backbone dihedral bin are the side-chain dihedral angles of the lowest energy "dipeptoid" from each cluster in that bin. The side-chain conformation of each final rotamer was sampled about the local minima until the energy increased by 0.5 Rosetta energy units (REU) to obtain an approximation of the width of the local energy minima. This local energy minima width is used as a proxy for the standard deviation of the side-chain conformations in a single rotamer bin.

QM Seeded Method. We devised an alternative methodology to use QM energy scans of a BBI model of the peptoid side chains as shown in Figure 1. The minimum energy wells identified from QM energy landscapes were used as starting points for lower level MM optimization and energy evaluation on a BBD model system. The BBI model containing each side chain is initialized in GAUSSIAN09 into discrete intervals spanning the entire $\chi_1-\chi_n$ (where *n* is the total number of χ angles) with a fixed ω backbone dihedral angle at either 0° for *cis* or 180° for *trans* conformations and allowed to geometrically minimize while keeping the ω dihedral fixed. The QM derived minima from those single point energy scans converge to small clusters. From each cluster, the χ angles that correspond to the lowest energy were recorded. This set of χ angles for both *cis* and *trans* conformations serves as the complete set of BBI energy wells. The BBI energy well χ dihedral angle coordinates were then initialized onto the BBD model in ROSETTA in the same range of backbone bins as the KMC protocol. The BBI energy well coordinates were then minimized using the ROSETTA **mm_std** scoring functions and their relative energies were used to determine rotamer probabilities assuming a Boltzmann distribution of the resulting energies. All geometry optimizations of the molecules in the BBI QM-derived minima scans were performed at the B3LYP/6-311+G(d,p) level of theory.

Rotamer Recovery of Oligo-Peptoid and Peptide−Peptoid Hybrid Structures. Rotamer recovery benchmarks tested the performance of the two rotamer libraries at reproducing the low energy packed side-chain conformations observed in experimental structures in both the presence (when applicable) and absence of the symmetry related partner molecules in the oligo-peptoid structures. A ROSETTA protocol was written to carry out fixed-backbone side-chain repacking using the **PackRotamersMover** followed by a comparison between the original and repacked side-chain conformations. The **PackRotamersMover** simultaneously repacks all side-chain positions using a Metropolis Monte Carlo simulated annealing procedure that attempts to find the lowest energy set of side-chain conformations given the current backbone conformation.[46] Calculations were performed with the **ex1**, **ex2**, and **ex3** command line flags set to "true"; and the **extrachi_cutoff** flag set to 0. These flags force ROSETTA to sample χ_1, χ_2, and χ_3 rotamers at their mean ± one standard deviation at all positions. In order to model only side-chain conformations described by the rotamer library, the **use_input_sc** flag is set to "false" to exclude the experimentally determined side-chain conformation of the input structures in sampling. A residue's side chain is considered predicted correctly if the χ angle of the repacked model was within ±20° of the position in the native structure.

■ RESULTS

Although peptoid oligomers can readily be synthesized to incorporate a wide diversity of side chains,[16,17] there are only a handful of experimentally determined peptoid structures. There
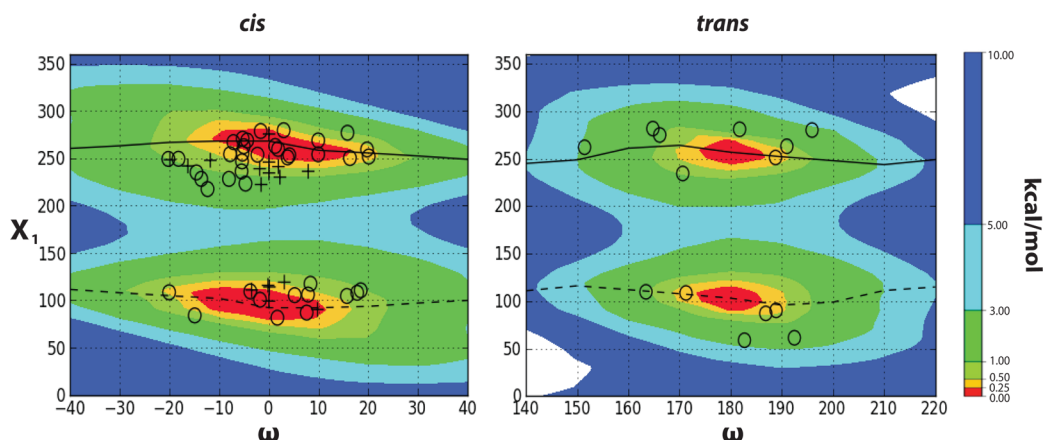
Figure 2. Effects of the ω dihedral angle on the χ_1 energy landscape. Energy landscapes were generated by fixing the dihedral angles of the TAB model to simultaneously achieve the desired χ_1 or ω. Cis-ω angles can be found on the left, trans-ω can be found at the right. Crystal structure data are shown as circles and crosses for angles and parameters found in cyclic and linear peptoid structures, respectively. In the trans-ω energy landscapes, crystal structure values for the "Nary" monomer are not plotted, as this parameter does not match the chemistry of the TAB model system. The minimum energy parameters are plotted across the full range of ω values as well as for positive (solid line) and negative (dashed line) χ_1 values. All molecules were minimized and energies evaluated at the B3LYP/6-311+G(d,p) level of theory, and heatmaps generated using the lowest energy for each plot as the zero kcal/mol baseline.

has yet to be a systematic analysis of side-chain conformations in all peptoid structures that explores side-chain conformations given all energetically feasible backbone conformations. Additionally, to determine if a rotameric treatment of peptoid side chains is appropriate, it is necessary to establish that the dihedral angle values of the experimental side-chain conformations cluster and that there is a multidimensional interdependence between the locations and frequency of those clusters.[43] Here we briefly describe our results for a small set of side chains for which there are sufficient experimental data to allow for proper validation. Following these case studies, we examine the performance of our rotamer library in ROSETTA in three ways. First, we explore our ability to fit existing structures by quantifying the distance between experimental side-chain conformations and the corresponding closest rotamers in our library. Second, we evaluate the performance of our rotamer library in the context of a peptoid design task by evaluating repacking of peptoid side chains within existing peptoid crystal structures. Lastly, we evaluate our ability to model peptoid side chain conformation at an experimentally validated protein-peptoid interface (in comparison to X-ray crystal structures of the interfaces). In all three cases, we achieved good performance for rotamers developed from both the quantum mechanically seeded (QMS) and k-means clustering (KMC) methods. This strongly indicates that peptoid side chain conformations can be approximated by a rotameric treatment and that our rotamer libraries are suitable for several design tasks.

Peptoid Side Chains are Dependent on the Preceding-ω Angle. Peptoids, unlike peptides, have greater flexibility around ω, with some monomer types readily populating both cis and trans (E/Z) ω angle conformations with a substantial range of deviation around the ideal angles of 0° and 180° for cis and trans, respectively.[41] The rotation of the preceding-ω torsion angle has been both predicted and observed to alter the preferred χ_1 value, as well as pyramidalization of the backbone nitrogen (χ_N) and backbone carbonyl carbon (χ_C) atoms.[44,47,48] To quantify the effect ω has on these side-chain conformations, and to justify development of a backbone dependent rotamer

library that includes this additional dihedral angle variability, we explored the ω-dependent energy landscapes.

In the development of rotamers based upon the TAB (Scheme 3), system we sought to ensure that rotamers developed using an inflexible amide bond model would be applicable for design in systems with slight deviations from ideal bond lengths, angles, and dihedral parameters. The rotamer libraries used by ROSETTA only include information about side-chain torsion angles with respect to the backbone torsion angle values. In order to use a rotameric treatment of peptoid side-chain conformations, the degrees of freedom that are not described in the rotamer library need to be relatively stable or invariant to perturbations of the backbone torsion angles. To verify that this was the case for peptoids, we quantified the relationships between the ω backbone dihedral angle and the χ_1 dihedral angle (Figure 2) as well as carbon (χ_C) and nitrogen (χ_N) Dunitz amide bond puckering parameters[49] (Figure S8).

From these energy landscapes, there are several notable dihedral angle dependencies. We found that the χ_1 rotamer energetic preferences for the TAB model were most significant (~0.5 kcal/mol) at extreme ω dihedral angle deviations from planarity. The χ_1 dihedral angle minima as denoted by the solid and dashed lines (Figure 2) had notable (~20°) deviations from 90° and −90°, dependent upon the ω dihedral angle. This result confirms the necessity to develop rotamer libraries dependent on not only the ϕ and ψ, but also on ω backbone dihedral angles, as the effects of ω deviations on χ_1 have now been quantified and have been found to be significant. The χ_N and χ_C Dunitz parameters varied as a linear function of ω. These puckering trends are built into the χ_1 energy landscapes, resulting in the observation that even with extreme ω dihedral angles and deviation of the amide bond from planarity, the χ_1 energetic preferences vary by only ~0.5° kcal/mol. This stability buttresses our confidence that idealized amide bonds are a reasonable starting approximation for ω-dependent peptoid rotamer libraries. From this result, we are confident that rotamer libraries that include an ω dependence will be able to accurately capture the energetic preferences of diverse peptoid oligomer species.
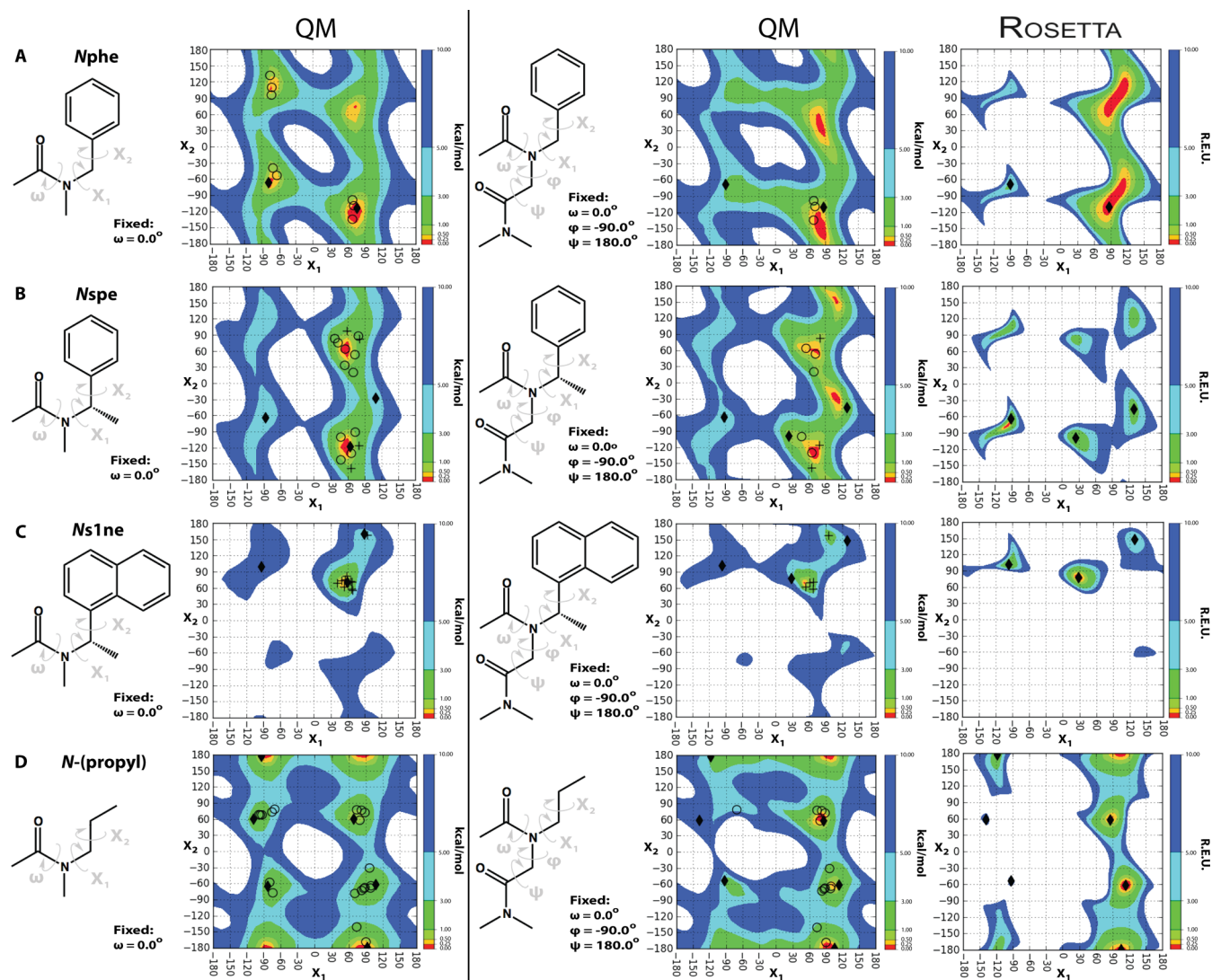
Figure 3. Fixed backbone rotamer energy landscapes for *Nphe*, *Nspe*, *Ns1ne*, and *N*-(propyl)-glycine side chains in a backbone-independent (BBI) and backbone-dependent (BBD) context. Crystal structure dihedral angle values are shown as circles and crosses for those observed in cyclic and linear peptoid structures, respectively. X-ray crystal dihedral angles for the different side chains are plotted only for the monomers in which the backbone dihedral angles were observed to be within 20° of the fixed backbone dihedral angles used in the energy landscape calculations. The minima from the BBI model landscapes (Figure S9) are represented as large diamonds in the BBI portion of the figure on the left. The diamonds on the right portion of the figure represent these rotamer positions in the context of the BBD model after ROSETTA **mm_std** energy function minimization. All landscapes underneath a QM header had energies evaluated at the B3LYP/6-311+G(d,p) level of theory. Landscapes under a ROSETTA header had energies evaluated using the **mm_std** energy function. Heatmaps were generated using the lowest energy as each plot's zero kcal/mol and zero REU (ROSETTA Energy Units) baseline for QM and ROSETTA, respectively.

Rotamer Library Creation. We used two protocols to generate backbone dependent (BBD) rotamer libraries for peptoid side chains in order to enable comparisons between approaches for identifying rotamers, scoring conformations, and modeling backbone-side-chain conformation interdependence. The first protocol is a modification of the method previously published[34] to calculate α-amino acid side-chain rotamer libraries, referred to as the KMC method. It uses the molecular mechanics (MM) based ROSETTA **mm_std** energy function in the context of a BBD molecule to evaluate rotamer energies. Previous studies[25,41,44,50] using quantum mechanics (QM) have shown a complex interaction between the peptoid side chain and backbone. While QM is accurate, it is also computationally intensive and cannot solely be used to create a full rotamer library or for side-chain repacking and design calculations. Our second method is a new rotamer library

creation protocol that uses input from QM calculations carried out on backbone-independent (BBI) molecules and is referred to as the QMS method. The QMS method then passes these QM-BBI minima to ROSETTA to estimate interactions with the backbone. Thus, each method uses a different strategy to reduce the complexity of the problem and arrive at a protocol with computational efficiency sufficient to allow calculation of rotamer libraries for multiple side chains. There are more than 200 peptoid side chains that are synthetically feasible;[17] however, only 9 different side chains have been used in experimentally determined peptoid structures. It is therefore essential that both protocols are general methods that do not incorporate or require structural information from experimentally determined peptoid structures as training data. We tested these two methods to determine if our rotamers, in conjunction with the MM based ROSETTA **mm_std** energy function, could
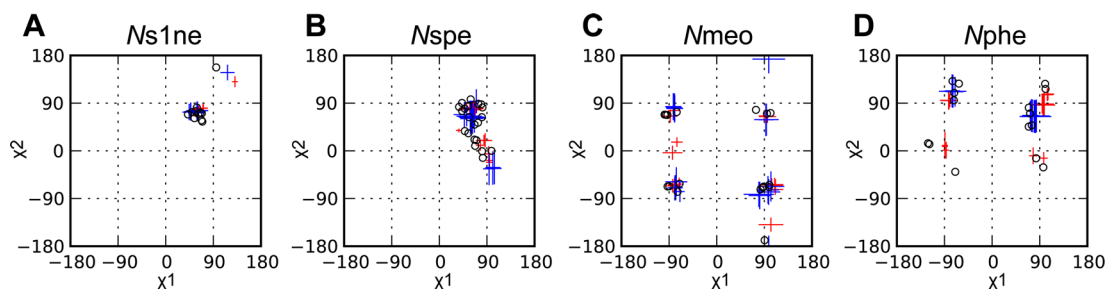
Figure 4. Rotamer library coverage plot for *N*phe, *N*s1ne, *N*meo, and *N*spe peptoid side chains. Interpolated χ torsions and standard deviations of the closest rotamer in the rotamer library based on the backbone dihedral angles of each experimental point are shown as crosses, where the center of the cross is at the mean and the length represents ± 1 standard deviation. Rotamers for the k-means clustering (KMC) method are shown as red crosses and quantum mechanically seeded (QMS) method are shown in blue. Experimental χ_1 and χ_2 values are shown as black circles.

accurately capture the behavior of peptoid side chains to the extent required by tools developed for protein modeling. We show that the two methods, despite taking different approaches, ultimately find similar rotamers. A discussion of the rotameric states of the side-chain conformations observed in the current set of peptoid structures and how they compare to the side-chain conformations of the rotamer libraries produced here are included in the Supporting Information. Additionally, an excerpt of the side-chain dihedral angles from the rotamer library are included in Supporting Information Tables S1−S4.

The energy landscape generated in the initial steps of the QMS protocol uses the BBI model (Scheme 4). This minimal model was chosen due to the fact that QMS single point energy evaluation of the energy landscape including the backbone ϕ and ψ torsions for all possible dihedral angles is computationally intractable. The reduced representation contains all of the side-chain atoms but only the ω torsion angle of the preceding residue. To investigate if this model is sufficient, we computed side-chain dihedral (χ_1 and χ_2) energy landscapes of four common side chains with BBD "dipeptoid" models at common low energy backbone conformations using QM and the ROSETTA **mm_std** energy function and compared them to the landscape of BBI models (Figure 3). Most notable is the absence of the χ_1 minima near $-90°$ that are present in the BBI model energy landscape but absent in the BBD energy landscape for the four common side chains. The absence is the result of steric interaction between the Cβ1 of the side chain and the C atom of the backbone which has a fixed ϕ dihedral of $-90°$. If the ϕ angles are fixed at $90°$, we observe an absence of χ_1 minima near $90°$. These results can be rationalized by the similar repulsive effects observed in the *syn*-pentane model system.[51] The loss of the $-90°$ minima seen in the backbone-dependent energy landscapes is analogous to the repulsive effects observed in *syn*-pentane which has been extrapolated to explain forbidden rotamers at certain ϕ and ψ dihedral angles of amino acids. Additionally, the appearance of the **m0°** and **p0°** rotamers of *N*spe and *N*phe in the BBD molecule in peptoid structures indicates that the BBI screen is not always successful in capturing the complete ensemble of side-chain conformations observed in peptoid structures. The QMS protocol is also limited to two χ angles, as a complete screen of side chains with many rotatable bonds is computationally intensive and often intractable with QM. Differences between *cis* and *trans* BBI models show that while the relative energy varies, the location of the minima remain similar between the two (Figure S9). The minima from the BBI model landscape found as small clustered circles in Figure S9 are represented as large diamonds in the BBI portion of Figure 3.

These minima are then initiated onto a BBD model and the model is allowed to minimize using linear gradient minimization and the ROSETTA **mm_std** scoring function. The diamonds on the BBD portion of Figure 3 represent these minimized rotamer positions in the presence of the backbone model. It can also be observed that the QM and MM BBD energy landscapes closely resemble one another, with only minor differences.

Rotamer Library Coverage of Experimentally Observed Side-Chain Conformations. ROSETTA and other computational protein modeling packages use side-chain dihedral angles in rotamer libraries to discretize the search for low energy side-chain conformations (protein repacking) or sequences (protein design) for a given backbone conformation. An accurate rotamer library will contain side-chain dihedral angle values close to values observed in experimentally determined structures. Rotamer libraries should be succinct for computational efficiency, but also sufficiently comprehensive to enable sampling of a large fraction of energetically accessible conformations.

To test the completeness of the rotamer libraries produced by the KMC and QMS rotamer library creation protocols, we carried out rotamer library "coverage" tests. These tests calculate the RMSD (in degrees) between the experimentally observed side-chain rotamer conformation and the closest rotamer in the given rotamer library. Results of the rotamer library coverage tests for the four frequently observed side chains are shown in Figure 4 and Table 1. Results of the other

Table 1. Averaged RMSD (in degrees and angstroms) from Experimentally Determined Peptoid or Peptide Side Chain Conformations and the Closest Rotamer in the Rotamer Libraries

monomer type	no. of χ	total	KMC[a]	QMS
*N*phe	2	15	**20.48°** (0.35 Å[b])	37.78° (0.43 Å)
*N*meo	3	17	26.39° (0.39 Å)	**17.90°** (0.32 Å)
*N*spe	2	21	**14.60°** (0.24 Å)	20.52° (0.33 Å)
*N*s1ne	2	11	11.71° (0.30 Å)	**10.68°** (0.27 Å)
monomer type	no. of χ	total		Dunbrack 2002[32]
Phe	2	924[c]		10.95° (0.17 Å)
Met	3	1039		14.42° (0.24 Å)

[a] Lower values within each group are shown in bold. [b] All non-hydrogen atoms in the monomer were used to calculate the RMSD. [c] Positions from the Top 8000 data set[52] with less than eight neighbors; two residues are considered neighbors if their neighbor atoms (Cα for glycine, Cβ for all others) are within 10 Å of each other.

Table 2. Summary of Rotamer Recovery Rate after Repacking of Oligo-Peptoid Structures Using KMC or QMS Rotamer Libraries with Symmetry Related Crystal Partners "Present" or "Absent"

| | totals | | KMC | | | | QMS | | | |
| | | | present | | absent | | present | | absent | |
	χ_1	χ_2	χ_1	χ_2	χ_1	χ_2	χ_1	χ_2	χ_1	χ_2
totals	95	74	53	25	58	28	50	28	65	25
percent (%)[a]			66	41	61	38	62	48	71	35

[a]Percent rotamer recovery "absent" crystal contacts totals have been adjusted to account for structures determined by NMR.
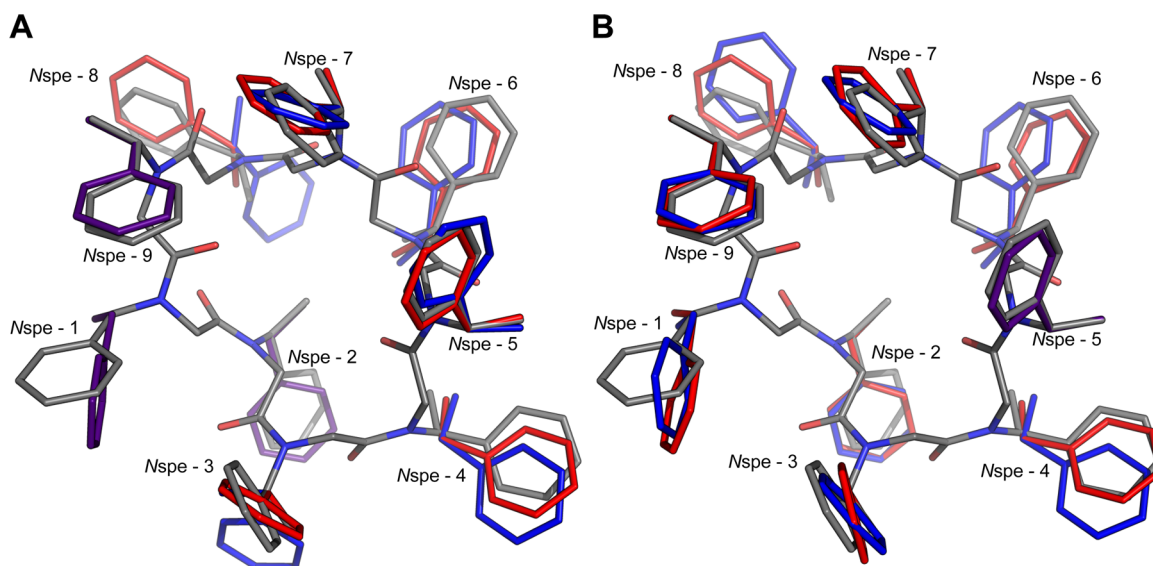

Figure 5. Peptoid data bank structure 12AC1-9-C and side-chain conformations after being repacked with (A) KMC rotamer libraries or (B) the QMS rotamer libraries. Experimental side-chain conformations are shown in gray, repacked side chains in blue, and repacked in the context of the symmetry related crystal partners in red. Positions for which the same rotamer was chosen in both contexts are shown in purple.

experimental side chains are shown in Figures S10−S14 and Table S5. For comparison, these tests were additionally carried out for phenylalanine and methionine side chains in protein structures in the Top 8000 data set[52] using the Dunbrack 2002 BBD rotamer library, Tables 1 and S7.

For each of the four most frequent peptoid side chains, either the KMC or QMS rotamer libraries contained rotamers with angles that are, on average, within less than 20° of experimental side chain values. For the Nspe side chain, only the **p90°** and **p0°** rotamers are experimentally observed and accurately modeled by rotamers created with both the KMC and QMS method. The experimental points occupy a wide energy valley that spans from a χ_2 of 90° to −30°. The KMC method performs better than the QMS as it is able to find a low probability rotamer in this valley while the QMS method predicts **p0°** rotamers closer to a χ_2 of −30°. For the Nmeo side chain, the experimental conformations adopt the traditional **m**, **p**, and **t** positions. The χ_3 dihedral angle values did not form tight clusters in the KMC protocol (data not shown). This results in a relatively large RMSD value (Table 1) despite χ_1 and χ_2 values being accurately predicted (Figure 4C). For the Nphe side chains, the RMSD value for the KMC rotamers is just over the 20° threshold while the QMS is significantly higher at ∼38°. The BBI screen of the QMS method misses the high energy **m0°** and **p0°** rotamers (Figure 3A), and the QMS rotamer library does not include these conformations. The QM energy landscape with the backbone present shows an elongated energy valley for χ_2 (Figure 3A). The five experimental examples with χ_2 near 0° are missed by the

QMS method and contribute to the high RMSD in Table 1. The three experimental points near the **m0°** rotamer are also significantly different from the values in the KMC library. Deviations in χ_1 can arise from pyramidalization which can greatly affect the positioning of the atoms making up the χ_1 dihedral angle, potentially influencing the χ_1 calculated value. When the experimental points with a χ_2 near 0° are omitted, the QMS rotamers have almost the same RMSD to the experimental values as the KMC rotamers for **m90°** and **p90°** rotamers (18.25° and 18.71°, respectively). For the Ns1ne side chain, both the KMC and QMS protocols perform as well as the Dunbrack 2002 library for protein data. The large steric bulk of the naphthyl group interacting with the $C\beta2$ atom of the Ns1ne side chain and peptoid backbone restricts the allowed conformations of the side chain. Only the **pp** rotamer is observed in the experimental data set, and both methods predict this rotamer accurately.

With few exceptions, rotamers observed in peptoid structures are found in the rotamer libraries produced by both methods. Both the KMC and QMS protocols produce similar rotamers with similar dihedral angles. The KMC protocol suitably evaluates longer side chains and is able to find side-chain conformations that involve backbone interactions such as the Nphe rotamers with χ_2 near 0°.

The Dunbrack 2002 rotamer library for the 20 canonical peptide amino acids performs better than our rotamer libraries perform on peptoid side chains. However, compared to the Top 8000 data set,[52] there are far fewer examples of peptoid structures than protein. Additionally, the data set employed for

the protein comparison is heavily pruned to only include the highest quality structures available; an option we do not have for peptoids.

Rotamer Recovery of Oligo-Peptoid Structures. ROSETTA has been developed and parametrized to repack globular protein structures. We investigated if the combination of the peptoid rotamer libraries and the **mm_std** scoring function have sufficient discriminatory power to recapitulate the side-chain conformations in the experimentally determined structures. We therefore undertook side-chain conformation recovery benchmarks similar to those employed in the early development of protein design methodologies.[53]

Each example in the set of ROSETTA compatible peptoid structures was repacked with ROSETTA using rotamer libraries from the KMC and QMS protocols and in the presence (where applicable) or absence of crystal contacts from symmetry related partners. The predicted side-chain dihedral angles of the repacked structures were compared to those in the experimental structure. A χ angle is judged to be correctly predicted ("recovered") if it is within 20° of the experimental value. Results of the rotamer recovery benchmark in structures containing only peptoid residues are shown in Table 2 and Figure 5.

Rotamer recovery rates in proteins improve with additional context about the environment the side chain is in. For surface positions, that additional context can be provided by the atoms from neighboring chains in the symmetery related cyrstalographic neighbors.[54] The surrounding atoms in a protein's core also provide additional context and can help determine correct rotamer position. Previous studies on proteins[34] found that ROSETTA achieved an over all rotamer recovery of 75% for χ_1 and 53% for $\chi_1 + \chi_2$ using the **mm_std** energy function and the Dunbrack 2002 rotamer library. A recovery of 59% for χ_1 and 37% for $\chi_1 + \chi_2$ was achieved for surface positions, and a recovery of 91% for χ_1 and 71% for $\chi_1 + \chi_2$ was achieved for core positions using the same energy function and rotamer library. The increased recovery of protein cores strongly suggests that, for a given position, the influence of surrounding side chains can enhance the discretization of low energy side-chain conformations. In the currently available set of peptoid structures, the number of neighbors a given side chain has is more comparable to the surfaces rather than cores of proteins. Both the KMC and QMS rotamer libraries are able to correctly predict the χ_1 conformations of more than 60% of peptoid positions both in the absence and presence of crystal structure contacts (Table 2). The KMC and QMS rotamer libraries achieve rates of peptoid side-chain recovery comparable to the recovery rate of the Dunbrack 2002 library for protein side chains at surface positions.

Our ability to recover correct rotamers is dependent on the quality of the rotamer library coverage. The 12AC1-9-C structure, an *N*spe 9-mer, has the highest rate of side chains recovered (Figure 5) because the rotamers produced by the KMC and QMS protocols have a low averaged RMSD compared to the experimental side chain conformations for *N*spe (Table 1). In contrast, the 12AB4-16-M structure contains only *N*meo and *N*ary side chains and has the lowest fraction of rotamers recovered in the set. The rotamer library coverage for the *N*meo and *N*ary side chains is more complete relative to *N*spe (Tables 1 and S5), and the effect is that we poorly predict the side-chain conformations within the 12AB4-16-M structure.

To get a better understanding of how ROSETTA will behave in repacking a peptoid side chain in the core of a globular protein or buried at protein–protein interfaces, we carried out rotamer recovery benchmarks in the context of the neighboring peptoid molecules in the solid state defined by the crystallographic symmetry transformations (Table 2). The addition of crystallographic partners has been shown to increase the rate of rotamer recovery at protein surface positions.[54] Although not a perfect analogue of a protein's hydrophobic core, increasing the number of neighboring residues through the addition of crystal contacts reduces the number of conformations assessable to the given peptoid position. Additionally, crystal contacts can direct the side chain into conformations that are lower in energy as a result of the additional contacts. This allows ROSETTA to choose a rotamer closer to those observed in the crystal structures. For example, *N*spe-4 and *N*spe-8 monomers in the peptoid data bank structure 12AC1-9-C are both correctly predicted by both the KMC and QMS rotamer libraries. However, the angles of the selected conformations are closer to the values in the experimental structure when crystal contacts are included in rotamer repacking. This effect is highlighted in Figure 5 with the side-chain conformation predicted with crystal partners (red) closer to the experimental conformation (gray) than without the crystal information (blue). There are currently too few structures to determine if crystal contacts direct side chains into off-rotamer conformations. However, for the two available NMR solution structures, ROSETTA has a χ_1/χ_2 recovery of 67%/75% for KMC and 80%/75% for QMS.

Conformational Analysis of Four Common Peptoid Side Chains Supports Rotameric Treatment. Our ability to accurately model peptoid side chain conformations with a rotameric treatment in rotamer recovery benchmarks supports the notion that peptoids are indeed rotameric. Like peptides, each peptoid side chain is rotameric at varying levels as a result of complex side chain to backbone intraresidue and steric interactions. Overall, we find that the currently available set of experimental side-chain conformations are sufficiently modeled with our predicted rotamer conformations. To more thoroughly evaluate the degree to which peptoids are rotameric will likely require additional peptoid structures with greater numbers of side-chain-side-chain contacts, tighter packing, and a more diverse palate of side chains. However, with the currently available set of ROSETTA-compatible peptoid data bank structures, we find that experimental side-chain conformations cluster well and that those clusters correspond to minima found in QM and ROSETTA **mm_std** energy landscapes. It is clear that some rotamers will simply not be observed due to steric clashes with the backbone; other predicted rotamers have not been observed due to the small size of the current database of peptoid structures. This initial study indicates that similar to peptides, peptoids also exhibit rotamer preferences. Furthermore, this finding suggests that protein modeling tools can be readily adapted to accommodate them.

Rotamer Recovery of Peptoid–Peptide Hybrid Structures. Nguyen and co-workers have deposited three structures of SH3 domains bound to inhibitory peptides in which each peptide has a single proline position mutated to a different peptoid side chain.[23,24] These three structures provide us an opportunity to test our ability to recover native rotamers in hybrid design contexts. Structure 1B07 contains two chains (labeled A and C in the deposited structure), while 2SEM and 3SEM contain four chains each, two pairs of protein/peptide

interactions (A/C and B/D, respectively). As with the rotamer recovery of the oligo-peptoid structures, each structure here was repacked and the side-chain dihedral angles were compared to those in the experimental structure. Results of the rotamer recovery benchmark in structures of peptoid/peptide hybrids are shown in Table S9 and Figure S15.

ROSETTA is able to recover the rotamers of the 1B07 and 2SEM structures using both the KMC and QMS rotamer libraries. We are not able to recover the rotamer of the peptoid side chain from the 3SEM structure. ROSETTA places the side chain in an alternative conformation (data not shown). The peptoid side chain in the 3SEM structure branches at the second side chain atom and makes few contacts in the crystal structure. Additionally, the average B-factors of the atoms in the 3SEM side chains are greater than 40, indicating uncertainty in the exact position of the peptoid side chain in this experimental structure (Table S9). For these reasons, 3SEM may not represent a suitable test of side chain repacking. We exhibit good performance for both structures with well-resolved peptoid side chains, but recognize that the small sample size prevents us from generalizing further.

■ DISCUSSION

We present a general method for creating rotamer libraries needed for rational design of peptidomimetic oligomer structures. We apply this method to the peptoid backbone and show performance is comparable to protein side-chain rotamer libraries derived from statistical analysis of the Protein Data Bank (PDB) for protein surface positions. This pipeline relies on MM and QM simulations in lieu of statistical analysis because far fewer crystal structures of peptoids exist than for proteins. Given the reliance on physics-based methods, we expect this method can be applied to several other diverse peptidomimetic scaffolds (such as β-peptides, D-amino acid, and hybrid oligomeric systems). A notable advantage of this method is that it can be used to build rotamer libraries for any specified side chain. This is demonstrated by the development of rotamers for over 50 peptoid side chains (shown in Figures S1−S7) that are capable of being incorporated via standard peptoid synthesis protocols.

Comparisons between QM evaluations of peptoid side-chain conformations and our rotamers show good agreement between the QMS and KMC rotamer library construction pipelines. Our comparisons with QM suggest we capture key features of the side-chain conformational landscape. We also find agreement with the side-chain conformations observed in X-ray crystal and NMR structures of peptoid oligomers (Figure 4). There are currently too few experimentally determined peptoid structures to derive peptoid rotamer libraries by statistical analysis. The currently available peptoid structures are of small oligomers (<20 residues) and are dominated by crystal contacts and local structure interactions (comparable to protein surface positions). We show that our rotamers agree with experimental side-chain conformations with RMSD values comparable to best-in-class protein rotamer libraries for α-amino acids at surface positions (Figure 4 and Table 1).

A large number of modifications to the ROSETTA design framework were required to enable peptoid design with these rotamer libraries (described in the Supporting Information); most notably, allowing for the use of BBD rotamer libraries that include preceding-ω in addition to ϕ and ψ. These modifications to the ROSETTA design procedure allowed us to evaluate our performance on repacking tasks, and again we find that these rotamer libraries will be sufficient for peptoids and hybrid peptoid-protein design tasks (such as designing peptoids to interrupt protein−protein interfaces). Despite the ROSETTA energy function being optimized for biological molecules in aqueous media, it performs surprisingly well at reproducing the side-chain conformations of relatively short oligo-peptoid structures in nonaqueous media. This indicates that the side-chain conformations of peptoids are primarily determined through local interactions. Adding peptoid design capabilities to ROSETTA allows access to kinematics, optimization, and scoring methods that enable a vast array of design and modeling tasks for peptoid, peptoid−protein, and peptoid−nucleic-acid systems. These rotamer library development methods are also extendable to other noncanonical backbones and peptidomimetic scaffolds. Future work will include adding capabilities to model and design several other peptidomimetic oligomer scaffolds.

A key remaining challenge not addressed here, is to model mixed oligomeric systems such as oligomers containing α-amino acids and peptoids. Additional study is required to determine if rotamer libraries derived individually for peptoid and α-amino acids will perform well in these hybrid settings.[55] In cases where a peptide side chain precedes a peptoid side chain, both side chains would be separated by only two bonds along the backbone and we speculate that this mixed system would require rotamer libraries specific to the joint between the two oligomeric systems. For cases in which peptoid side chains are N-terminal to peptide, the proximal side chains will be separated by four bonds and it is likely that the rotamers derived in this study would perform well in this mixed setting. Other key areas for future work include the need for developing better methods to estimate the unfolded state energies (sometimes referred to as the "reference energy") as well as new methods for dealing with larger side chains.

As we design, build, and refine peptoids, we will increase the diversity and number of structures and thus increase our ability to score and judge peptoid designs. We thus intend to bootstrap our way toward design capabilities for both peptoid and mixed protein−peptidomimetic systems that approach pure protein design in accuracy and breadth of application. This work represents the first iteration of this process.

■ ASSOCIATED CONTENT

Ⓢ Supporting Information

Additional methods and results detailing the selection of side chains incorporated in to ROSETTA, selection of oligo-peptoid structures, modifications to ROSETTA, calculation of ω versus χ_C and ω versus χ_N energy landscapes, conformational analysis of experimental peptoid side-chain conformations, additional rotamer library coverage analysis, complete list of rotamer recovery results for oligo-peptoid and peptide−peptoid hybrid strucutres, and code and methods desemination (Supporting Information 1). Rotamer library coverage plots for for each individual position in the set of oligo-peptoid strucures (Supporting Information 2). Energies and coordinates of all structures that underwent geometry optimization (Supporting Information 3). This material is available free of charge via the Internet at http://pubs.acs.org.

■ AUTHOR INFORMATION

Corresponding Author

bonneau@nyu.edu

Author Contributions

[⊥]P.D.R. and T.W.C. contributed equally to this publication.

■ REFERENCES

(1) Koga, N.; Tatsumi-Koga, R.; Liu, G.; Xiao, R.; Acton, T. B.; Montelione, G. T.; Baker, D. *Nature* **2012**, *491*, 222−227.

(2) Bida, J.; Das, R. *Curr. Opin. Struct. Biol.* **2012**, *22*, 457−466.

(3) King, N. P.; Sheffler, W.; Sawaya, M. R.; Vollmar, B. S.; Sumida, J. P.; Andr, I.; Gonen, T.; Yeates, T. O.; Baker, D. *Science* **2012**, *336*, 1171−1174.

(4) Gellman, S. H. *Acc. Chem. Res.* **1998**, *31*, 173−180.

(5) Dunbrack, R. L., Jr. *Curr. Opin. Struct. Biol.* **2002**, *12*, 431−440.

(6) Petersson, E. J.; Schepartz, A. *J. Am. Chem. Soc.* **2008**, *130*, 821−823.

(7) Cao, J.; Kline, M.; Chen, Z.; Luan, B.; Lv, M.; Zhang, W.; Lian, C.; Wang, Q.; Huang, Q.; Wei, X.; Deng, J.; Zhu, J.; Gong, B. *Chem. Commun.* **2012**, *48*, 11112−11114.

(8) Tosovska, P.; Arora, P. S. *Org. Lett.* **2010**, *12*, 1588−1591.

(9) Lee, B.-C.; Chu, T. K.; Dill, K. A.; Zuckermann, R. N. *J. Am. Chem. Soc.* **2008**, *130*, 8847−8855.

(10) Kwon, I.; Wang, P.; Tirrell, D. A. *J. Am. Chem. Soc.* **2006**, *128*, 11778−11783.

(11) Reinert, Z. E.; Lengyel, G. A.; Horne, W. S. *J. Am. Chem. Soc.* **2013**, *135*, 12528−12531.

(12) Huang, M. L.; Ehre, D.; Jiang, Q.; Hu, C.; Kirshenbaum, K.; Ward, M. D. *Proc. Natl. Acad. Sci. U.S.A.* **2012**, *109*, 19922−19927.

(13) Maayan, G.; Ward, M. D.; Kirshenbaum, K. *Proc. Natl. Acad. Sci. U.S.A.* **2009**, *106*, 13679−13684.

(14) Raveendra, B.; Wu, H.; Baccala, R.; Reddy, M.; Schilke, J.; Bennett, J.; Theofilopoulos, A.; Kodadek, T. *Chem. Biol.* **2013**, *20*, 351−359.

(15) Utku, Y.; Dehan, E.; Ouerfelli, O.; Piano, F.; Zuckermann, R. N.; Pagano, M.; Kirshenbaum, K. *Mol. BioSyst.* **2006**, *2*, 312−317.

(16) Zuckermann, R. N.; Kerr, J. M.; Kent, S. B. H.; Moos, W. H. *J. Am. Chem. Soc.* **1992**, *114*, 10646−10647.

(17) Culf, A. S.; Ouellette, R. J. *Molecules* **2010**, *15*, 5282−5335.

(18) Crapster, J. A.; Guzei, I. A.; Blackwell, H. E. *Angew. Chem., Int. Ed.* **2013**, *52*, 5079−5084.

(19) Butterfoss, G. L.; Yoo, B.; Jaworski, J. N.; Chorny, I.; Dill, K. A.; Zuckermann, R. N.; Bonneau, R.; Kirshenbaum, K.; Voelz, V. A. *Proc. Natl. Acad. Sci. U.S.A.* **2012**, *109*, 14320−14325.

(20) Seo, J.; Barron, A. E.; Zuckermann, R. N. *Org. Lett.* **2010**, *12*, 492−495.

(21) Huang, M. L.; Shin, S. B. Y.; Benson, M. A.; Torres, V. J.; Kirshenbaum, K. *ChemMedChem* **2012**, *7*, 114−122.

(22) Chongsiriwatana, N. P.; Patch, J. A.; Czyzewski, A. M.; Dohm, M. T.; Ivankin, A.; Gidalevitz, D.; Zuckermann, R. N.; Barron, A. E. *Proc. Natl. Acad. Sci. U S.A.* **2008**, *105*, 2794−2799.

(23) Nguyen, J. T.; Porter, M.; Amoui, M.; Miller, W. T.; Zuckermann, R. N.; Lim, W. A. *Chem. Biol.* **2000**, *7*, 463−473.

(24) Nguyen, J. T.; Turck, C. W.; Cohen, F. E.; Zuckermann, R. N.; Lim, W. A. *Science* **1998**, *282*, 2088−2092.

(25) Shah, N. H.; Butterfoss, G. L.; Nguyen, K.; Yoo, B.; Bonneau, R.; Rabenstein, D. L.; Kirshenbaum, K. *J. Am. Chem. Soc.* **2008**, *130*, 16622−16632.

(26) Stringer, J. R.; Crapster, J. A.; Guzei, I. A.; Blackwell, H. E. *J. Am. Chem. Soc.* **2011**, *133*, 15559−15567.

(27) Huang, M. L.; Benson, M. A.; Shin, S. B. Y.; Torres, V. J.; Kirshenbaum, K. *Eur. J. Org. Chem.* **2013**, *2013*, 3560−3566.

(28) Naffin, J. L.; Han, Y.; Olivos, H. J.; Reddy, M.; Sun, T.; Kodadek, T. *Chem. Biol.* **2003**, *10*, 251−259.

(29) Nam, K. T.; Shelby, S. A.; Choi, P. H.; Marciel, A. B.; Chen, R.; Tan, L.; Chu, T. K.; Mesch, R. A.; Lee, B.-C.; Connolly, M. D.; Kisielowski, C.; Zuckermann, R. N. *Nat. Mater.* **2010**, *9*, 454−460.

(30) Vollrath, S. B. L.; Hu, C.; Bräse, S.; Kirshenbaum, K. *Chem. Commun.* **2013**, *49*, 2317−2319.

(31) Levine, P. M.; Craven, T. W.; Bonneau, R.; Kirshenbaum, K. *Org. Biomol. Chem.* **2013**, *11*, 4142−4146.

(32) Dunbrack, R. L.; Cohen, F. E. *Protein Sci.* **1997**, *6*, 1661−1681.

(33) Shapovalov, M. V.; Dunbrack, R. L. *Structure* **2011**, *19*, 844−858.

(34) Renfrew, P. D.; Choi, E. J.; Bonneau, R.; Kuhlman, B. *PLoS One* **2012**, *7*, e32637.

(35) Gfeller, D.; Michielin, O.; Zoete, V. *J. Comput. Chem.* **2012**, *33*, 1525−1535.

(36) Shandler, S. J.; Shapovalov, M. V.; Dunbrack, J.; DeGrado, W. F. *J. Am. Chem. Soc.* **2010**, *132*, 7312−7320.

(37) Leaver-Fay, A.; et al. An Object-Oriented Software Suite for the Simulation and Design of Macromolecules. In *Methods in Enzymology*; Johnson, M. L., Brand, L., Eds.; Computer Methods, Part C; Academic Press: New York, 2011; Vol. *487*; pp 545−574.

(38) Leh, J.; Kirshenbaum, K. *Peptoid Data Bank*; http://www.nyu.edu/projects/kirshenbaum/Peptoid_Databank.html, 2012.

(39) Huang, K.; Wu, C. W.; Sanborn, T. J.; Patch, J. A.; Kirshenbaum, K.; Zuckermann, R. N.; Barron, A. E.; Radhakrishnan, I. *J. Am. Chem. Soc.* **2006**, *128*, 1733−1738.

(40) Drew, K.; et al. *PLoS One* **2013**, *8*, e67051.

(41) Butterfoss, G. L.; Renfrew, P. D.; Kuhlman, B.; Kirshenbaum, K.; Bonneau, R. *J. Am. Chem. Soc.* **2009**, *131*, 16798−16807.

(42) As agreed upon at the 8th Peptoid Summit, August 2012.

(43) Lovell, S. C.; Word, J. M.; Richardson, J. S.; Richardson, D. C. *Proteins: Struct., Funct., Bioinf.* **2000**, *40*, 389−408.

(44) Jordan, P. A.; Paul, B.; Butterfoss, G. L.; Renfrew, P. D.; Bonneau, R.; Kirshenbaum, K. *Peptide Sci.* **2011**, *96*, 617−626.

(45) Frisch, M. J. et al. *GAUSSIAN 09*, Revision A.1; Gaussian Inc.: Wallingford, CT, 2009.

(46) Kuhlman, B.; Baker, D. *Proc. Natl. Acad. Sci. U.S.A.* **2000**, *97*, 10383−10388.

(47) Armand, P.; Kirshenbaum, K.; Falicov, A.; Dunbrack, R. L., Jr.; Dill, K. A.; Zuckermann, R. N.; Cohen, F. E. *Folding Des.* **1997**, *2*, 369−375.

(48) Laursen, J. S.; Engel-Andreasen, J.; Fristrup, P.; Harris, P.; Olsen, C. A. *J. Am. Chem. Soc.* **2013**, *135*, 2835−2844.

(49) Winkler, F.; Dunitz, J. *J. Mol. Biol.* **1971**, *59*, 169−182.

(50) Paul, B.; Butterfoss, G. L.; Boswell, M. G.; Renfrew, P. D.; Yeung, F. G.; Shah, N. H.; Wolf, C.; Bonneau, R.; Kirshenbaum, K. *J. Am. Chem. Soc.* **2011**, *133*, 10910−10919.

(51) Dunbrack, R. L.; Karplus, M. *Nat. Struct. Mol. Biol.* **1994**, *1*, 334−340.

(52) Richardson, J. S.; Richardson, D. C. *Biopolymers* **2013**, *99*, 170−182.

(53) Leaver-Fay, A. et al. In *Methods in Enzymology*; A. E. Keating, Ed.; Methods in Protein Design; Academic Press: New York, 2013; Vol. *523*; pp 109−143.

(54) Krivov, G. G.; Shapovalov, M. V.; Dunbrack, R. L. *Proteins: Struct., Funct., Bioinf.* **2009**, *77*, 778−795.

(55) Butterfoss, G. L.; Drew, K.; Renfrew, P. D.; Kirshenbaum, K.; Bonneau, R. Conformational Preferences of Peptide−Peptoid Hybrid Oligomers. *Pept. Sci.* 2014, accepted.